FINAL REPORT

The manganese (II) dependent transcriptome of the citric acid overproducer fungus *Aspergillus niger* (NN 128867)

Levente Karaffa, DSc
Department of Biochemical Engineering, University of Debrecen

MAIN PROJECT

Introduction, scientific background

Citric acid (2-hydroxypropane-1,2,3-tricarboxylic acid; citrate) is amongst the most important bulk products of industrial biotechnology. Global production of citrate is estimated at about 2.4 million tons in 2021, with a market volume > $2.5 billion. China accounts for over 60% of global citrate production. Due to the large citrate production plant currently being constructed in the Szolnok Industrial Park by a Chinese company, Hungary is soon becoming a major European citrate producer/exporter.

The application of citrate is based on its (1) acidity and buffer capacity, (2) palatability, (3) ability to chelate metal ions (Karaffa et al. 2001). Due to its pleasant taste and minimal toxicity, citrate is widely used as additive in foods and beverages. It is also able to complex heavy metal ions such as iron and copper, and is therefore applied in the stabilization of oils and fats against metal ion-catalysed oxidation (Kubicek and Karaffa 2006).

Citrate is the denominator intermediate of the ubiquitous citric acid (Szentgyörgyi-Krebs, or tricarboxylic) cycle, and thus occurs in almost every living organism. The discovery of its accumulation by the filamentous fungus *Aspergillus niger* led to the development of a large-scale submerged fermentation process which today accounts for 95% of the world's citrate production (Kubicek and Röhr 1986).

Citrate overflow requires a unique combination of several unusual nutrient conditions (very high concentrations of carbon source, H^+ and dissolved oxygen, and suboptimal concentrations of certain trace metals and phosphate), which synergistically influence the yield (Kubicek and Karaffa 2010). The pathways of citrate formation include glycolytic catabolism of D-glucose to two molecules of pyruvate, and their subsequent conversion to the precursors of citrate, i.e., oxaloacetate and acetyl-CoA. Yields can reach up to 95 % ($Y_{p/s}$), but they only exceed 66% when the carbon dioxide released in the pyruvate dehydrogenase reaction is not lost. Indeed, of the two molecules of pyruvate resulting from the glycolytic catabolism of glucose, one is converted to acetyl-CoA (by releasing one mole of carbon dioxide) and the other one to oxaloacetate (by fixing this one mole of carbon dioxide onto the second pyruvate; Karaffa and Kubicek 2003).

Manganese (II) ions and citrate overflow

Adjusting correct levels of the trace elements iron, zinc, copper, and manganese in the medium is a further critical precondition for high yield citrate production. Citrate production occurs only when these ions are present in very low concentrations. Of all the metal ions, manganese (II) ions (henceforth referred to as Mn) are the most critical, as concentrations as low as >5 ppb already reduce citrate accumulation by 20% (Kisser et al. 1980). Such concentrations are easily

introduced into the medium by other nutrients such as the carbon source, and therefore Mn must be removed from the feedstock (Karaffa et al., 2021).

Mn-deficiency has multiple effects on *A. niger* physiology, including fungal morphology: mycelia grown under manganese-deficient conditions form small, dense, vacuolated and branched pellets with thickened cell walls. This morphology improves rheology and oxygen transfer (Cox and Thomas 1992).

Citrate export from the cytosol is an ATP-dependent process, which is significantly increased in mycelia grown under Mn-deficiency. On the other hand, citrate permease can only import the Mn-chelated citrate. Apart from blocking citrate uptake, shifting the saturated : unsaturated fatty acid ratio of the plasma membrane and significantly influencing morphology, Mn-deficiency additionally interferes with the metabolism of *A. niger* by causing an impairment of protein and DNA synthesis, inhibiting triglyceride and phospholipid synthesis and altering the polysaccharide concentration of the cell wall. Overall, despite its paramount significance in citrate production, the molecular mechanisms of Mn-deficiency in citrate accumulation are still unclear.

Fundamental hypothesis, research strategy

Our hypothesis was that multiple factors are involved in the diverse phenotype associated with Mn deficiency. To test the involvement of genetic elements, in collaboration with our Canadian partners at Concordia University (Quebec, Montreal), we analysed the transcriptome of the high citrate producer, genome-sequenced *A. niger* strain (ATCC 2270) by deep RNA sequencing from cultures that are cultivated at three different Mn concentrations. Subsequently, a bioinformatics analysis targeting the differential gene expression was performed. These data were then used to identify genes which display an at least 2-fold up- or downregulation in dependence on the availability of Mn. Genes (or a selection of them) fulfilling these criteria were then investigated further by generating knock-out and/or overexpressing mutant strains employing the CRISPR/Cas9 gene editing technology (Nødvig et al. 2015) followed by phenotype analysis, with an emphasis on biomass formation, morphology and citrate production potential, as well as on the ability of Mn import from the liquid growth medium.

Materials and Methods developed/optimized for this project

At the onset of the research project, proper fermentation and analytical protocols were set up that enabled us to run fermentations with a specific molar citrate yield ($Y_{p/s}$) of > 0.8. We also set up an Image Analysis protocol to characterize the kinetics of the *A. niger* morphology, and developed methods for the determination of extracellular, intracellular and cellwall-bound Mn-concentrations by inductively coupled plasma quadrupole mass spectrometer (ICP-QMS). The operational adjustments undertaken to optimize the *A. niger* citric acid fermentation at lab-scale (6-L) to achieve specific molar yields > 0.8 – thereby mimicking true producing settings – were as follow:

- Inoculum concentration was raised from 8% to 12% (v/v). Mycelial inoculum was used, as opposed to conidiospores.
- Initial pH of the main fermentation was set at 2.5 (in contrast to the conventional value of 3.5).
- Initial stirring rate was fixed at 200 rpm, which resulted in DO levels > 80% in the first 24 hours. DO was subsequently controlled at 30% by the mechanical stirrer (200 – 900 rpm).

As for fungal morphology, it was defined in three forms – (a) the swollen hyphal fragments called yeast-like forms, (b) the filamentous hyphae and (c) the mycelial pellets that are spherical colonies of highly entangled hyphal biomass (Paul and Thomas, 1998). Morphology was investigated microscopically with an Axio-Vision AC quantitative image analyser system. To increase contrast and visibility, lactophenol cotton blue was added to the medium samples in a final concentration of 10 % (v/v). Stained samples were analyzed with a Zeiss AxioImager phase-contrast microscope, equipped with AxioCam MRc5 camera. Average cell- and average pellet diameters (also referred to as micro- and macro-morphology, respectively) were assessed with the AxioVision AC image analyser system processing at least 50 cells or 10 pellets for each liquid culture sample studied.

For the determination of Mn-concentrations in the liquid growth media, Inductively Coupled Plasma Quadrupole Mass Spectrometer (ICP-QMS; ThermoFisher Scientific, Bremen, Germany), equipped with Hexapole Collision Cell Technology (CCT) was used. A gas mixture of 7 % hydrogen and 93% helium was applied as collision/reaction gas at a flow rate of 6 ml min-1. The instrument was controlled by a PlasmaLab software (ver. 2.5.10.319, Thermo Fisher Scientific). Calibration curves were set up by appropriate dilutions of a mono-elemental Mn reference solution (1000 mg L^{-1} Mn(II), Scharlab S. L., Spain). Recovery was in the range of 95-100%. The samples were analyzed at m/z 55 for Mn(II) and m/z 103 for the internal standard element rhodium, which had a concentration of 20 µg L^{-1} in all solutions (Karaffa et al., 2015).

Results and Discussion

Leaching from the bioreactor – a new source of manganese contamination

Technical-scale production of citric acid predominantly uses stainless-steel tank fermenters, but glass bioreactors used for strain improvement and manufacturing process development also contain stainless steel components, in which Mn is an essential alloying element. For a long time, it had been suspected that during citric acid fermentations Mn leaches from the bioreactor into the growth media. Within this project, we demonstrated for the first time that such leaching indeed occurs, resulting in altered fungal physiology and morphology, and significant reduction of citric acid yields.

The experimental setup involved two glass bioreactors that share the same vessel geometry and working volume (4.5 L), their metal components are all made of 316L stainless steel (≤ 2% Mn-content), and both are equipped with a pair of six-blade Rushton-type disc turbine impellers of 60 mm diameter. However, Bioreactor A was newly purchased just before this study, while Bioreactor B was purchased 10 years ago, and have been extensively used ever since, resulting in visibly corroded metal surfaces.

Following a standard sterilization protocol in steam autoclaves, we performed parallel *A. niger* citric acid fermentations in the two bioreactors (A, B) under identical, optimized cultivation conditions. Despite of the apparent uniformity, pH, biomass, D-glucose- and citric acid concentrations as well as fungal morphology all significantly differed. Final fungal biomass concentration in Bioreactor B was approximately twice as high, being associated with higher overall specific growth rates for that culture (μ = 0.019 h^{-1} vs. 0.014 h^{-1}). Biomass in Bioreactor B grew significantly faster, reaching a 19 times higher concentration by 24 h relative to the value right after inoculation, corresponding to a specific growth rate of μ = 0.12 h^{-1}. In contrast, the same period in Bioreactor A saw a five-times increase in biomass only (μ = 0.067 h^{-1}). Citric acid accumulation and molar yield were, however, much higher in Bioreactor A than

in B ($Y_{p/s}$ = 0.4 ± 0.03 vs. $Y_{p/s}$ = 0.95 ± 0.02). Fungal morphology was also dissimilar: at the early stages (up to 120 h), morphology in Bioreactor A was characterized by the dominance of small, compact pellets and yeast-like cells – typical for a high-yield citric acid producing culture – as opposed to elongated hyphae in Bioreactor B, which is associated with non-producing conditions. In the later stages, cultures from the two bioreactors were getting more similar with a generally pellet-like morphology.

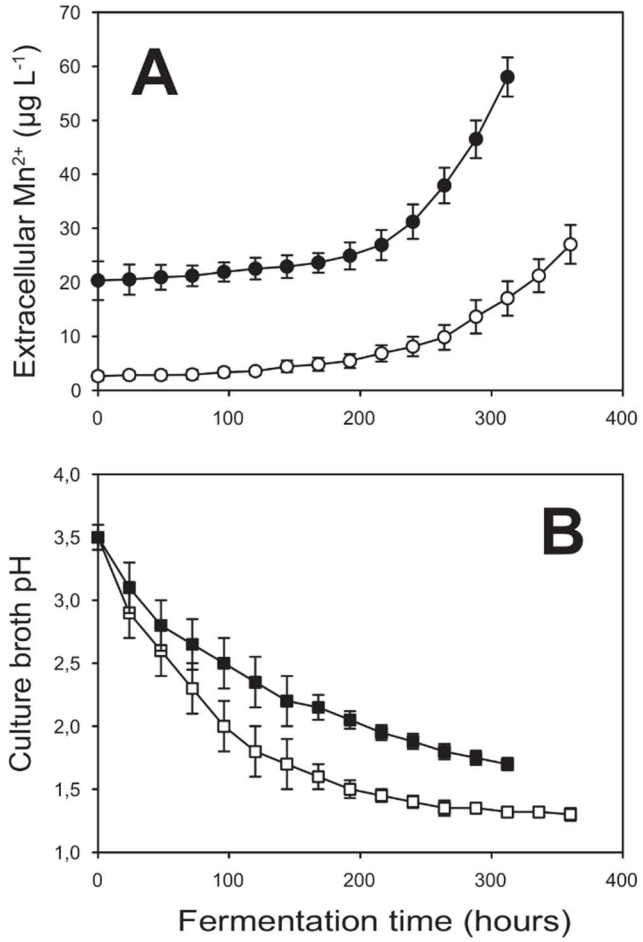

Figure 1. *Kinetics of extracellular manganese(II) ion concentration (**panel A**) and extracellular pH (**panel B**) for the A. niger cultures grown in the new Bioreactor A (empty symbols) and the old Bioreactor B (stuffed symbols).*

Profiles of pH were also different (**Figure 1B**). While cultures shared the same initial value (pH 3.5) that first rapidly and later more slowly decreased till the end of the fermentations, the final values were pH 1.3 for the high-yield culture as opposed to pH 1.6 in Bioreactor B.

As for the Mn-concentrations in the culture broth (**Figure 1A**), initial levels were always set at 2 µg L^{-1} prior to the sterilization. In the new and old bioreactor alike, elevated Mn-concentrations were detected after the sterilization (but prior to the inoculation) than before. The concentration increase – apparently prompted by the sterilization – was significantly larger in the old Bioreactor B than in the new Bioreactor A (0.55 µg L^{-1} vs. 18.29 µg L^{-1}). Following inoculation, time-course Mn-concentrations changes were monitored. Levels continuously increased with time, but the kinetics of changes was much different. In Bioreactor A, Mn-concentrations remained <5 µg L^{-1} for the first half of the fermentation, and afterwards they

increased steeply till the end. In contrast, Mn-concentrations in Bioreactor B started off from the elevated (inhibitory) level and thus they were in the inhibitory range in the course of the entire fermentation. Notably though, in the second half of the fermentation, Mn-levels steeply increased also in Bioreactor B, reaching a final concentration of almost 60 μg L^{-1}.

By comparing the kinetic profiles of the culture pH with that of the extracellular Mn-concentrations we noticed that in both bioreactors Mn-accumulation significantly increased when the pH of the culture broth fell below ~2.0. To investigate the relationship between pH and Mn-leaching, we filled Bioreactor A with either 10 mM or 100 mM phosphate-buffered Mn-free water. The results confirmed that the accumulation of Mn is pH-dependent: negligible between 3.0 and 2.2, started to increase at 2.0, and steeply accelerated below pH 2.0. This result in principle may have suggested that keeping extracellular pH at around 2.0 would prevent Mn-leaching. However, citric acid biosynthesis is known to be strongly influenced by the pH of the culture broth. Indeed, performing a citric acid fermentation with external pH control resulted in rather low ($Y_{p/s}$ = 50 %) molar yields even under otherwise optimized conditions, thus this strategy to counteract Mn-leaching was not considered further. In summary, we quantified Mn-leaching from the stainless steel components of bioreactors into the growth media during optimized *A. niger* citric acid fermentations, and identified heat sterilization and acidic culture pH as two of the underlying reasons.

Preventing manganese ion intake

As mentioned above, the Mn-concentration in the growth medium must be kept < 5 μg L^{-1}, which is less than the amount bound as contaminant to the carbon source. Consequently, Mn needs to be removed from the fermentation broth or counteracted by addition of other compounds. Another way to eliminate the detrimental effect of Mn on citric acid production is the modulation of the transport activity, thereby preventing these ions from being taken up. This was the strategy we have undertaken in the framework of this project.

The import of Mn into cells is mediated by transporters. The divalent metal transporter 1 (DMT1), a member of the NRAMP (Natural Resistance-Associated Macrophage Proteins) transporter family, is the primary Mn-transporter in mammalian cells. In *Saccharomyces cerevisiae*, two NRAMP transporters (named Smf1 and Smf2) are responsible for modulating intracellular Mn-levels.

A BLASTP search of the *A. niger* NRRL2270 genome with the *S. cerevisiae* Smf1p and Smf2p sequences as queries resulted in the identification of NRRL3_07789. The encoded protein comprises 575 amino acids and exhibits 58% amino acid identity with both yeast orthologues. This gene is present in the parent of NRRL2270, *A. niger* ATCC 1015, and also in the glucoamylase producer *A. niger* CBS 513.88. The corresponding proteins share 100% amino acid sequence identity. We concluded that neither NRRL3_07789 nor its genomic locus has been altered in proficient citric acid producing strains.

We constructed *A. niger* mutant strains in which NRRL3_07789 was either deleted or overexpressed under the starch-inducible glucoamylase (*glaA*) promotor. In the deletion strain, no NRRL3_07789 transcripts were found thus confirming the deletion of the gene. In contrast, the overexpressing strain exhibited increased NRRL3_07789 transcript level after 1 and 3 h in the Mn-limited medium. To demonstrate that NRRL3_07789 encodes a divalent metal ion transporter capable of Mn-transport, we first set up a system for measuring the rate of transport of Mn into the cells by monitoring the decrease of Mn concentration in the medium. *A. niger* exhibited a maximal intake rate of 10 ± 2 pmoles min^{-1} g_{DCW}^{-1} at 100 μg L^{-1} of Mn. Mn transport by the deletant strain at low concentrations of Mn (5 μg L^{-1}) occurred at a rate that was less than

6% of that of the parent strain, whereas at 1 mg L^{-1} the rate was 30% of that of the parent strain. The strain overexpressing NRRL3_07789, however, exhibited a 5-fold higher activity at 5 µg L^{-1} (13.3 pmoles $min^{-1}g_{DCW}^{-1}$), and this was increased to 22 and 24.9 pmoles $min^{-1}g_{DCW}^{-1}$ at 100 and 1000 µg Mn L^{-1}, respectively. Hence, measurement of the Mn intake rate of the two mutants confirmed the product of NRRL3_07789 is capable of Mn transport. We therefore proposed that NRRL3_07789 is a divalent metal ion transporter capable of high affinity Mn transport, and named it DmtA. Results also demonstrate that there must be at least one more transporter for Mn with lower affinity that contribute to a third of the intake rate at high Mn-concentrations.

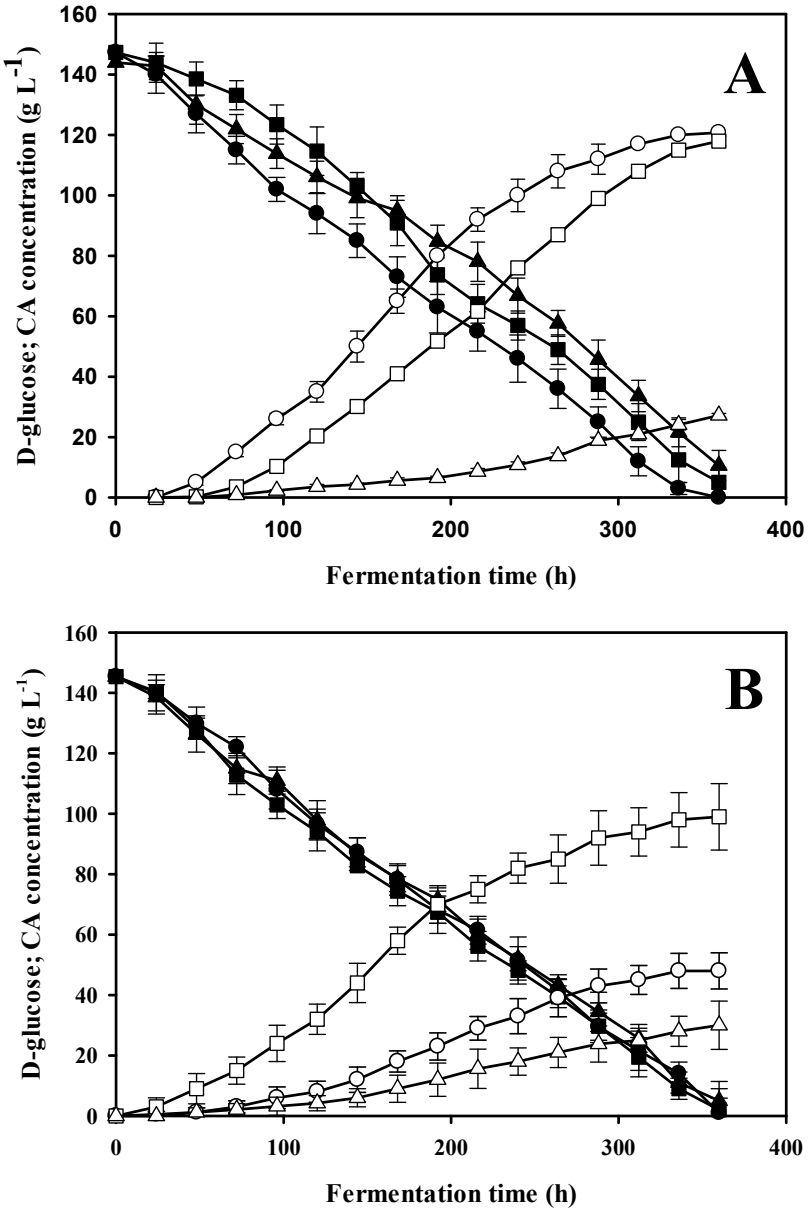

Figure 2. *Residual glucose content and citric acid production during A. niger citric acid fermentations at Mn-deficiency (5 µg L^{-1};* ***Panel A****) and Mn-sufficiency (100 µg L^{-1};* ***Panel B****). Filled symbols represent D-glucose concentrations, open symbols show citric acid concentrations (circle – NRRL2270, square – ΔmntA, triangle – mntAOE)*

To determine the effect of a loss of *dmtA* on citric acid production in the presence of Mn, we grew the parent strain, the *ΔdmtA* strain and the *dmtA*OE strain at two different Mn-concentrations, 5 and 100 µg $L^{-1,}$ in a citric-acid producing condition (**Figure 2**). At initial concentration of 5 µg L^{-1} Mn the parent strain produced 120 g L^{-1} citric acid after 350 h, which corresponds to a specific molar yield ($Y_{p/s}$) of 0.8. The *ΔdmtA* strain produced the same amount of citric acid as the parent strain, although with a delay of about 40 h, confirming that the absence of *dmtA* has no negative effect on citric acid production level. The *ΔdmtA* strain grew slower and accumulated only about a third as much biomass as the parent strain. Consequently, its specific citric acid production (g g^{-1} biomass) is higher than in the parent strain (17.1 vs 10 g g^{-1}).

The *dmtA*OE strain, in contrast, produced only 25-30 g L^{-1} citric acid under Mn-limiting conditions. This suggests that the enhanced expression of *dmtA* increases the intracellular Mn-concentration that shifts metabolism away from citric acid production. This is also reflected by the observation that the *dmtA*OE strain forms 5-fold more biomass at 5 µg L^{-1} than the parent strain (48 g L^{-1}).

Under high Mn-conditions (in the presence of 100 µg L^{-1}), D-glucose intake rates in the three cultures were not statistically different, whereas citric acid production was strongly influenced by mutations in *dmtA*. Citric acid production by the parent strain reached only 40-45 g L^{-1}, whereas *ΔdmtA* still accumulated about 100 g L^{-1}. This difference was even more dramatic when the specific production was compared (= 0.8 vs. 6.6 g g^{-1}) because – although the *ΔdmtA* accumulated three-times more biomass than under Mn-limitation – the parent strain still accumulated 2.5-fold as much biomass than *ΔdmtA*. Nevertheless, these data also reveal a considerable reduction in the cells ability to produce citric acid in the presence of 100 µg L^{-1} Mn, which cannot be fully prevented by the absence of the DmtA transporter.

Summarizing, we have identified and characterized a single NRAMP permease in *A. niger* (named DmtA) that has high sequence identity to both Smf1 and Smf2. We showed that manipulation of *dmtA* activity, either by gene deletion or overexpression, has a significant impact on the interplay between the extracellular Mn-concentration and citrate production in *A. niger*.

Only the first two days matter

We furthermore demonstrated that leaching of Mn from the bioreactor does not limit citric acid accumulation as long as it occurs in the late stages of the fermentation. At least under the conditions used in the experiments, Mn deficiency in the first 48 hours of the fermentation appear critical for citric acid overflow. This time-span may turn out to be strain- and technology dependent, but the results nonetheless indicate that the so-called “manganese effect” diminishes as fermentation progresses, mitigating the problem of Mn leaching from metal surfaces. The results also imply that once *A. niger* citric acid overflow commences due to the special cultivation conditions, it continues irrespective of the changing environment in the bioreactor. Indeed, the high initial concentration of D-glucose – considered one of the most critical elements of high-yield citric acid production – also gradually decreases as the fermentation progresses, but that does not seem to influence the sugar/acid conversion rate either. We thus hypothesized that the genes involved in the response to manganese deficiency are expressed at a very early stage of the cultivation.

Analysis of the manganese-dependent transcriptome

To test the hypothesis above, we sampled three parallel *A. niger* citric acid fermentations at 24, 48 and 72 hours, and the frozen biomass was sent to a commercial company for deep RNA sequencing. Following RNA isolation, DNAse treatment, Quality Control of total RNA samples, poly(A) enrichment, cDNA synthesis and Illumina Library preparation using barcodes as well as equimolar pooling according to library quantification measurements, a bioinformatics analysis was undertaken. The bioinformatics analysis comprised mapping of the reads to the reference genome, determination of gene expression and statistical analysis. These data were used to identify genes which display an at least 2-fold up- or downregulation in dependence on the availability of manganese(II) ions. Genes (or a selection of them) fulfilling these criteria are / shall be investigated further by generating knock-out and/or overexpressing mutant *A. niger* strains employing the CRISPR/Cas9 gene editing technology.

From the biochemical evaluation of the *A. niger* manganese transcriptome, we have concluded that Mn-deficiency appears to turn on the transcription of secreted and membrane-located proteins. In order to see whether the differential expression (i.e., under Mn+ and Mn- conditions) is statistically supported, we have performed Gene Ontology (GO) enrichment analysis on all genes in the 24, 48 and 72 hrs samples, by using the clusterprofiler package (**Figure 3A, B, C**).

BP = Biological Process; CC = Cellular Component; MF = Molecular Function

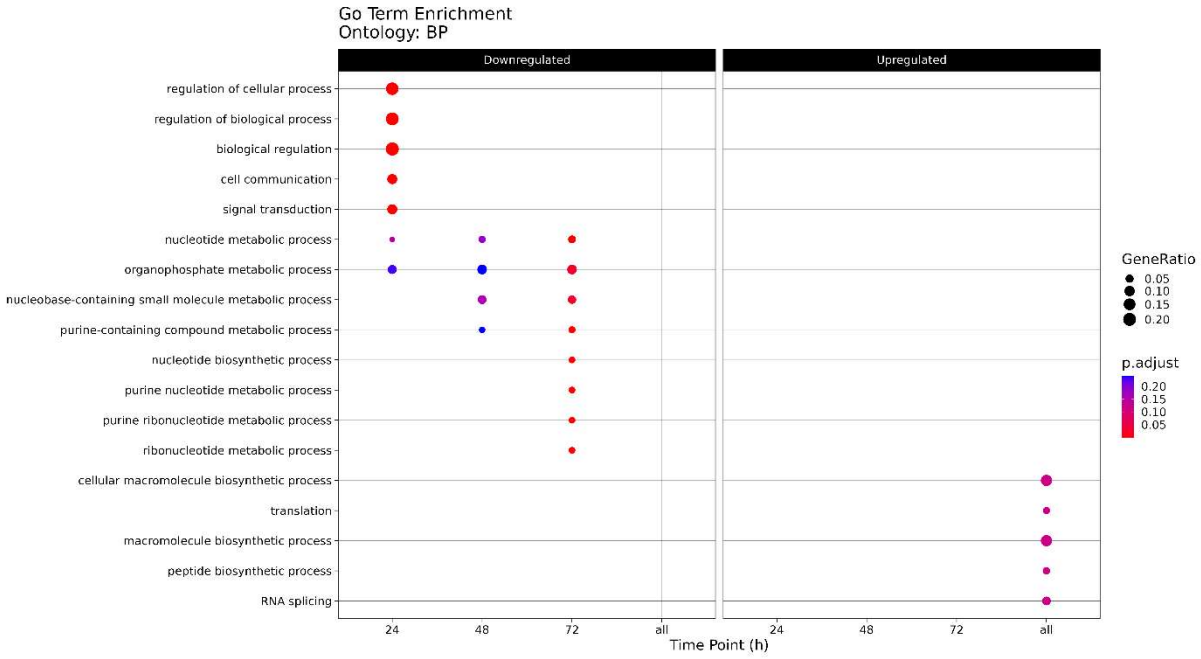

***Figure 3A**. GO enrichment graphics produced for Biological Processes-related gene products*

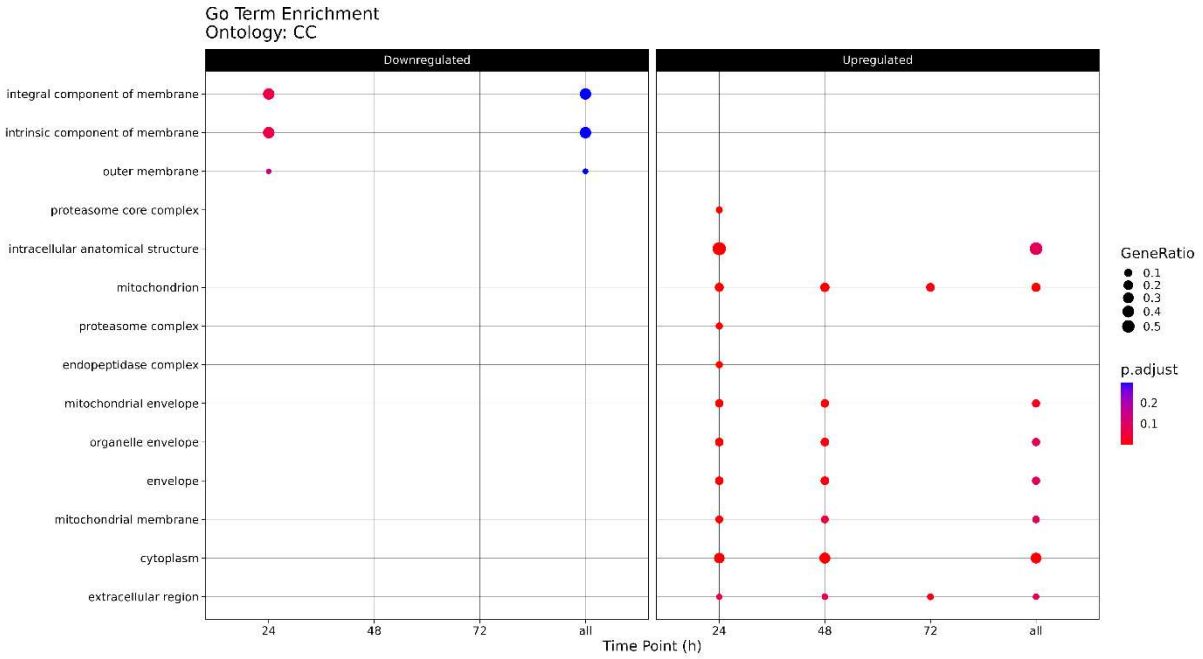

***Figure 3B**. GO enrichment graphics produced for Cellular Component-related gene products*

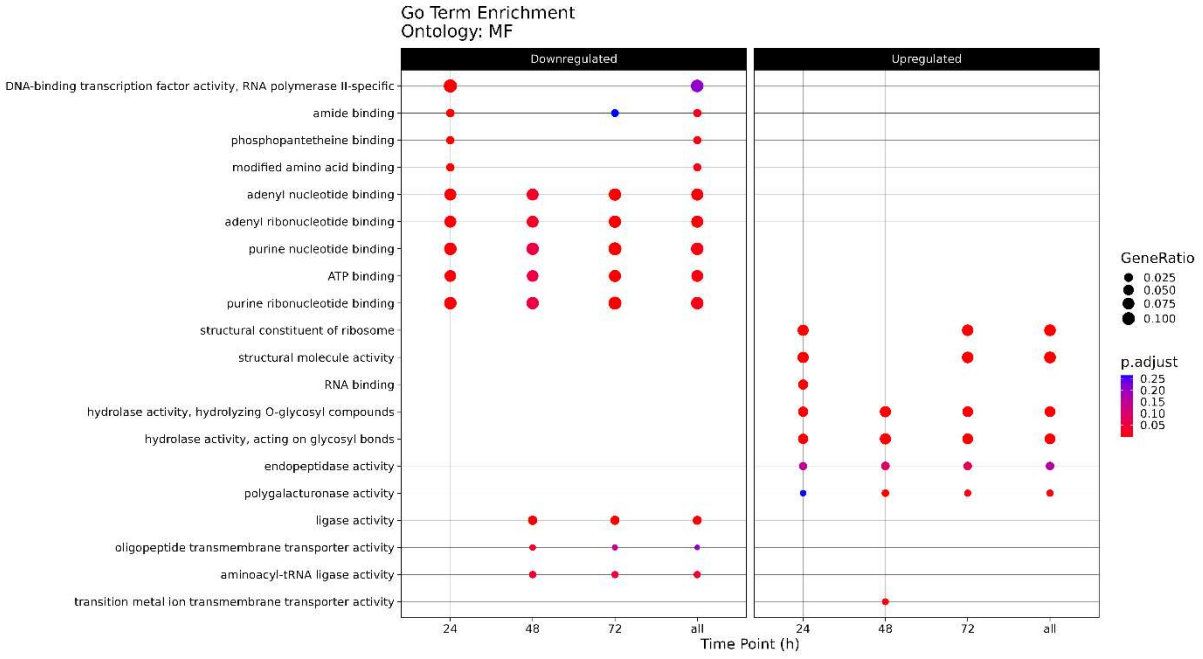

***Figure 3C**. GO enrichment graphics produced for Molecular Function-related gene products*

The most promising candidate gene appeared to be *cexA*, encoding a citrate exporter protein responsible for secreting citric acid from the cytosol into the culture broth (Steiger et al., 2019). This transmembrane protein belongs to the group of drug H^+-antiporter and major facilitator superfamily. While importing H^+ ions, CexA simultaneously exports citrate into the culture medium. We have deleted and overexpressed cexA; experiments with the two mutant strains suggest that CexA does play a major role in the manganese effect (**Table 1**). Importantly,

increased expression of cexA occurs at the two early time-points (i.e., 24 and 48 hrs), while expression returns close to that of the reference strain after 72 hrs of cultivation.

Time (h)	Citric acid (g L^{-1})		DCW (g L^{-1})		$Y_{p/s}$ (%)	
	OE cexA	NRRL 2270	OE cexA	NRRL 2270	OE cexA	NRRL 2270
0	64.2 ± 3.9	52.2 ± 3.2	34.9 ± 4.2	49.1 ± 3.8	0.43 ± 0.04	0.35 ± 0.03
24	80.6 ± 4.8	65.7 ± 4.2	26.1 ± 3.1	42.4 ± 3.0	0.54 ± 0.04	0.44 ± 0.03
72	123.9 ± 5.1	106.0 ± 5.1	10.4 ± 1.1	19.2 ± 2.7	0.83 ± 0.04	0.71 ± 0.03
120	128.4 ± 3.5	119.4 ± 3.8	9.1 ± 1.0	12.3 ± 1.4	0.86 ± 0.04	0.80 ± 0.04
196	128.4 ± 3.3	128.4 ± 3.5	9.2 ± 0.8	9.3 ± 1.0	0.86 ± 0.03	0.86 ± 0.04

Table 1. *Maximal volumetric citric acid yields, maximal fungal biomass (DCW) concentrations and specific molar citric acid yields (Yp/s) of cultures of an Aspergillus niger mutant strain constitutively expressing cexA (OE cexA) and the NRRL 2270 hyper-producer strain (control). The initially manganese(II) ion deficient cultures were supplemented with 100 μg L-1 Mn(II) at 0, 24, 72 and 120 h, respectively. Initial D-glucose concentrations were 140 g* L^{-1}.

Perspectives

Most recently, we have created a double mutant *A. niger* strain (ΔdmtA; ΔglaA::cexA) where overexpression of cexA is governed by the *glaA* promoter, and the manganese transporter gene is missing. This mutant is expected to secrete citrate at an increased rate while simultaneously, the Mn-effect is diminished. Preliminary phenotype analysis at 6-L scale laboratory fermenters indicates that this mutant produces statistically the same amount of citrate in the presence as in the absence of Mn, at very high ($Y_{p/s}$ >95%) molar yields.

AN IMPORTANT SIDE-PROJECT: MECHANISMS OF ITACONIC ACID OVERFLOW

Itaconic acid (2-methylenesuccinic acid) is an unsaturated, weak dicarboxylic acid (pK_a = 3.83 and 5.41) produced by *Aspergillus terreus*. It was described as a thermal decomposition product of citric acid. Indeed, the biosynthetic pathway of itaconic acid resembles that of citric acid, the latter acid being a direct precursor of the former. The only difference is that citric acid in *A. terreus* is further metabolized via *cis*-aconitate to itaconate by *cis*-aconitate decarboxylase. Citrate is likewise synthesized from oxaloacetate and acetyl-CoA, while oxaloacetate is synthesized from pyruvate by anaplerotic CO_2 fixation in the cytosol. It is then shuttled into mitochondria by a specific antiporter in exchange for *cis*-aconitate. Itaconic acid – formed upon *cis*-aconitate decarboxylation – is secreted out of mycelia by a specific cell membrane transporter. Genes encoding these three enzymes (and a fourth one encoding a transcription factor) constitute the „itaconate gene cluster" in the *A. terreus* genome.

The presence of the conjugated double bond of the methylene group of itaconate allows polymerization both by addition and condensation. Esterification of the two carboxylic groups with different co-monomers is also possible (Kuenz et al. 2012). These diverse properties have led to a variety of applications in the pharmaceutical, architectural, paper, paint, and medical industries such as as plastics, resins, paints, synthetic fibers, plasticizers, detergents. The US Department of Energy in 2004 assigned itaconic acid as one of the top 12 most promising building block chemicals for bio-based economy.

Itaconic acid production is exclusively performed by submerged fermentation in batch mode (Cavallo et al. 2017). Regarding scale, vessel types, inoculation protocols, critical process parameters, medium composition, the upstream of the *A. terreus* itaconic acid fermentation is much similar to the *A. niger* citric acid production. Itaconic acid is thus produced on molasses or hydrolyzed starch, applied at very high (> 12%, w/v) concentrations. The process is strongly aerobic, and extremely sensitive to the presence of Mn. For this reason we extended our research on the *A. niger* manganese effect towards itaconic acid production by *A. terreus*.

Hypothesises to test

On technical scale, itaconic acid is produced from glucose-containing complex carbon sources. However, stiff competition with food applications keeps the fermentation industry searching for cheap, renewable raw materials to be utilized. Hence, research interests over the more efficient utilization of non-food, lignocellulosic plant biomass are soaring for a long time now (Cunha da Cruz et al., 2018). Lignocellulose is a complex polymer of hexose and pentose monomers, whereby D-xylose is the most abundant pentose. However, D-glucose and D-xylose as well as D-xylose and L-arabinose partially interfere with each other's uptake and metabolism, and thus investigation of their combined conversion will only result in scientifically valid data if the metabolism of these sugars in the absence of the others is understood first. Since itaconic acid in *A. terreus* is formed by the same metabolic pathway as citric acid in *A. niger*, it was not unreasonable to assume that the physiological requirements for itaconic production from D-xylose (and consequently the fermentation parameters) would be similar to those on D-glucose. There is a major difference, however, because the fungal catabolism of D-xylose occurs via the pentose catabolic pathway (Khosravi et al. 2018) and only at later stages feeds its intermediates into glycolysis.

We have therefore tested whether two landmark nutritional requirements of the *A. terreus* itaconic acid overflow on D-glucose – Mn(II) ion deficiency and high concentration of the carbon source – also occur in a similar fashion on D-xylose as a sole source of carbon, and whether their respective optimization would give as high molar yields from D-xylose as from D-glucose. Subsequently, the ability of Cu(II) ions to alleviate the negative effect of Mn(II) ions on itaconic acid fermentations have been tested on carbon sources that constitute lignocellulose – that is, D-xylose, L-arabinose, D-glucose and D-fructose.

Results and Discussion

A carbon and energy balance for itaconic acid formation was established, which is 0.83 moles/mole D-xylose. The effect of Mn-ions on itaconic acid formation was similar to that on D-glucose and maximal yields were obtained below 3 µg/L Mn(II) ions, which were, however, only 0.63 moles of itaconic acid per mole D-xylose. In contrast to the case on D-glucose,

increasing D-xylose concentration over 50 g/L did not change the above yield. By-products such as xylitol and α-ketoglutarate were found, but they cumulatively remained below 2% of the concentration of D-xylose. Mass balance of the fermentation with 110 g/L D-xylose revealed that > 95% of the carbon from D-xylose was accounted as biomass, itaconic acid and the carbon dioxide released in the last step of itaconic acid biosynthesis. These data show that the efficiency of biomass formation is the critical parameter for itaconic acid yield from D-xylose under otherwise optimal conditions. In the presence of higher external Mn-concentrations itaconic acid yield decreases and biomass formation is favored, but this could be mitigated by increasing the Cu(II) concentration in the medium. *A. terreus* displayed a very high tolerance to Cu(II) which, however, decreased when Mn-availability became increasingly limiting. High (> 75%) specific molar itaconic acid yields always coincided with an "overflow-associated" morphology, characterized by small compact pellets (<250 μm diameter) and short chains of "yeast-like" cells that exhibit increased diameters relative to the elongated cells in growing filamentous hyphae. At low concentrations (≤1 mg/L) of Cu(II) ions, Mn-deficiency did not prevent filamentous growth. Mycelial- and cellular morphology progressively transformed into the typical overflow-associated one when external Cu(II) concentrations increased, irrespective of the available Mn. Our results indicate that copper ions are relevant for overflow metabolism and should be considered when optimizing D-xylose based itaconic acid fermentation in *A. terreus*.

References

Cavallo E, Charreau H, Cerrutti P, Foresti ML (2017): Yarrowia lipolytica: a model yeast for citric acid production. FEMS Yeast Res 17:.fox084.

Cox PW, Thomas CR (1992): Classification and measurement of fungal pellets by automated image analysis. Biotechnol. Bioeng. 39: 945–952.

Cunha da Cruz J, Machado de Castro A, Camporese Sérvulo EF (2018): World market and biotechnological production of itaconic acid. 3 Biotech. 8: 138.

Karaffa L, Díaz R, Papp B, Fekete E, Sándor E, Kubicek CP (2015): A deficiency of manganese ions in the presence of high sugar concentrations is the critical parameter for achieving high yields of itaconic acid by *Aspergillus terreus*. Appl. Microbiol. Biotechnol. 99: 7937-44.

Karaffa L, Fekete E, Kubicek CP (2021): The Role of Metal Ions in Fungal Organic Acid Accumulation. Microorganisms. 9:1267.

Karaffa L, Sándor E, Fekete E, Szentirmai A (2001): The biochemistry of citric acid accumulation by *Aspergillus niger*. Acta Microbiol. Immun. Hung. 48: 429-441.

Karaffa L. Kubicek CP (2003): *Aspergillus niger* citric acid accumulation: do we understand this well-working black box? Appl. Microbiol. Biotechnol. 61: 189-196.

Khosravi C, Battaglia E, Kun RS, Dalhuijsen S, Visser J, Aguilar-Pontes MV, et al. (2018). Blocking hexose entry into glycolysis activates alternative metabolic conversion of these sugars and upregulates pentose metabolism in *Aspergillus nidulans*. BMC Genomics, 19:214.

Kisser M, Kubicek CP, Röhr M (1980): Influence of manganese on morphology and cell-wall composition of *Aspergillus niger* during citric acid fermentation. Arch. Microbiol. 128: 26–33.

Kubicek CP, Karaffa L (2006): Organic Acids. In: *Basic Biotechnology*, 3rd Edition (Ratledge C., Kristiansen B., eds.), 359-381. Cambridge University Press, Cambridge, UK.

Kubicek CP, Karaffa L (2010): Citric acid processes. *Encyclopedia of Industrial Biotechnology: Bioprocess, Bioseparation, and Cell Technology* (Michael C. Flickinger, ed.) 3: 1652-1658. John Wiley & Sons, Inc., Hoboken, N.J., U.S.A.

Kubicek CP, Röhr M (1986): Citric acid fermentation. CRC Crit. Rev. Biotechnol. 3: 331–373.

Kuenz A, Gallenmüller Y, Willke T, Vorlop KD (2012): Microbial production of itaconic acid: developing a stable platform for high product concentrations. Appl. Microbiol. Biotechnol. 96: 1209–16.

Nødvig CS, Nielsen JB, Kogle ME, Mortensen UH (2015): A CRISPR-Cas9 system for genetic engineering of filamentous fungi. PLoS One Art. No. e0133085.

Paul GC, Thomas CR (1998): Characterisation of mycelial morphology using image analysis. Adv. Biochem. Eng. Biotechnol. 60:1-59.

Steiger MG, Rassinger A, Mattanovich A, Sauer M (2019): Engineering of the citrate exporter protein enables high citric acid production in *Aspergillus niger*. Metab. Eng. 52: 224-231.

SCIENTIFIC PAPERS BASED ON THIS PROJECT

1) **Karaffa L.**, Kubicek C.P. (2019): Citric acid and itaconic acid accumulation: variations of the same story? *Applied Microbiology and Biotechnology,* 103: 2889-2902.
Impact factor: 3.670 (Q1)

2) Kolláth I.S., Molnár Á.P., Soós Á., Fekete E., Sándor E., Kovács B., Kubicek C.P., **Karaffa L.** (2019): Manganese deficiency is required for high itaconic acid production from D-xylose in *Aspergillus terreus*. *Frontiers in Microbiology*, 10: 1589.
Impact factor: 4.259 (Q1)

3) Fejes B., Ouedraogo, J-P., Fekete E., Sándor E., Flipphi M., Soós Á., Molnár Á.P., Kovács B., Kubicek C.P., Tsang A., **Karaffa L.** (2020): The effects of external Mn^{2+} concentration on hyphal morphology and citric acid production are mediated primarily by the NRAMP-family transporter DmtA in *Aspergillus niger*. *Microbial Cell Factories*, 19: 17.
Impact factor: 5.328 (Q1)

4) Sándor E., Kolláth I.S., Fekete E., Bíró V., Flipphi M., Kovács B., Kubicek C.P., **Karaffa L.** (2021): Carbon-source dependent interplay of copper and manganese ions modulates the morphology and itaconic acid production in *Aspergillus terreus*. *Frontiers in Microbiology*, 12: 680420. **Impact factor: 5.640 (Q1)**

5) **Karaffa L.**, Kubicek C.P. (2021): Production of Organic Acids by Fungi. In: Zaragoza, O. (ed). Encyclopedia of Mycology. vol. 2, pp. 406–419. Oxford: Elsevier.

6) **Karaffa L.**, Fekete E., Kubicek C.P. (2021): The role of metal ions in fungal organic acid accumulation. *Microorganisms*, 9: 1267. **Impact factor: 3.864 (Q2)**

7) Fekete E., Bíró V., Márton A., Bakondi-Kovács I., Németh Z., Sándor E., Kovács B., Fábián I., Kubicek C.P., Tsang A., **Karaffa L.** (2022): Bioreactor as the root cause of the "manganese effect" during *Aspergillus niger* citric acid fermentations. *Frontiers in Bioengineering and Biotechnology*, 10: 935902. **Impact factor: 6.064 (Q1)**

8) Flipphi M., Márton A., Bíró V., Ág N., Sándor E., Fekete E., **Karaffa L.** (2023): mutations in the second alternative oxidase gene: a new approach to group *Aspergillus niger* strains. *Journal of Fungi*, 9: 570. **Impact factor: 5.724 (Q1)**

SCIENTIFIC PAPERS ASSOCIATED WITH THIS PROJECT (GRANT NUMBER INDICATED)

9) Németh Z, Kulcsár L, Flipphi M, Orosz A, Aguilar-Pontes MV, De Vries RP, **Karaffa L**, Fekete E (2019): L-Arabinose induces D-galactose catabolism via the Leloir pathway in *Aspergillus nidulans*. *Fungal Genetics and Biology*, 123: 53-59.
Impact factor: 3.314 (Q1)

10) Kavalecz N., Ág N., **Karaffa L.**, Scazzocchio C., Flipphi M., Fekete E. (2019): A spliceosomal twin intron (stwintron) participates in both exon skipping and evolutionary exon loss. *Scientific Reports*, 9: 9940. **Impact factor: 4.011 (D1)**

11) Ág N., Kavalecz N., Pénzes F., **Karaffa L.**, Scazzocchio C., Flipphi M., Fekete E. (2020): Complex intron generation in the yeast genus *Lipomyces*. *Scientific Reports*, 10: 6022. **Impact factor: 4.379 (Q1)**

12) Kovács C., Csótó A., Pál K., Nagy A., Fekete E., **Karaffa L.**, Kubicek C.P., Sándor E. (2021): The biocontrol potential of endophytic *Trichoderma* fungi isolated from Hungarian grapevines. Paper I. Isolation, identification and *in vitro* studies. *Pathogens,* 10: 1612. **Impact factor: 3.492 (Q2)**

13) Fekete E., Pénzes F., Ág N., Scazzocchio C., Flipphi M., **Karaffa L.** (2021): Internally symmetrical stwintrons and related canonical introns in *Hypoxylaceae* species. *Journal of Fungi*, 7: 710. **Impact factor: 5.816 (D1)**

14) MENG J., NÉMETH Z., PENG M., FEKETE E., GARRIGUES S., LIPZEN A., NG V., SAVAGE E., ZHANG Y., GRIGORIEV I.V., MÄKELÄ M.R., **KARAFFA L.**, DE VRIES R.P. (2022): GalR, GalX and AraR co-regulate D-galactose and L-arabinose utilization in *Aspergillus nidulans. Microbial Biotechnology,* 15:1839-1851. **Impact factor: 5.813 (Q1)**

15) Fekete E., Pénzes F., Ág N., Ág-Rácz V., Sándor E., Scazzocchio C., Flipphi M., **Karaffa L.** (2022): Unique and Repeated Stwintrons (Spliceosomal Twin Introns) in the *Hypoxylaceae*. *Journal of Fungi*, 8: 397. **Impact factor: 5.816 (D1)**

16) Csótó A., Kovács C., Pál K., Nagy A., Peles F., Fekete E., **Karaffa L.**, Kubicek C.P., Sándor E. (2023): The biocontrol potential of endophytic *Trichoderma* fungi isolated from Hungarian grapevines. Paper II. Grapevine stimulation. *Pathogens*, 12: 2. **Impact factor: 4.531 (Q2)**

17) Zabiák A., Kovács C., Takács F., Pál K., Peles F., Fekete E., **Karaffa L.**, Mihály K., Flipphi M., Sándor E. (2023): *Diaporthe* and *Diplodia* species associated with walnut (*Juglans regia L.*) in Hungarian orchards. *Horticulturae*, 9: 205. **Impact factor: 2.923 (Q1)**

18) Csótó A., Nagy A., Laurinyecz N., Nagy Z.A., Németh Cs., Németh E.K., Csikász-Krizsics A., Rakonczás N., Fontaine F., Fekete E., Flipphi M., **Karaffa L.**, Sándor E. (2023): Hybrid *Vitis* cultivars with American or Asian ancestries show higher tolerance towards Grapevine Trunk Diseases. *Plants*, 12: 2328. **Impact factor: 4.658 (Q1)**